Vol. 48, No. 2 (2026) 379-391, DOI: 10.24874/ti.2175.04.26.06

Tribology in Industry

www.tribology.rs

RESEARCH

Tribological Analysis of Traction Enhancement in Rope-Plate Conveyors Using Shock-Absorbing Idlers

Kadirbek Baizhumanov[a], Turgara Tusseyev[a], Mergen Zhumanov[a], Ayezhan Turdaliev[b]

[a]*Farabi Kazakh National University, Department of Thermophysics and Technical Physics, 71 Al-Farabi Avenue, Almaty, Kazakhstan,*
[b]*International University of Transportation and Humanities, Zhetysu – 1, Almaty, Kazakhstan.*

Keywords:

Rope-plate conveyor
Tribology
Coefficient of friction
Abrasive wear
Contact pressure
Traction ropes
Frictional interaction

* Corresponding author:

K.D. Baizhumanov
E-mail: kadirbek_79@mail.ru

Received: 13 April 2026
Revised: 19 May 2026
Accepted: 5 June 2026

A B S T R A C T

The article presents the results of an analytical and experimental study of the tribological characteristics of a rope-plate conveyor intended for transporting large-sized and abrasive materials. The frictional interaction between traction ropes and the supporting-gripping elements of the load-carrying belt using shock-absorbing supporting idlers and pressure roller supports, which ensure redistribution of contact pressure and stabilization of the adhesion regime, is considered.

The effective coefficient of friction under operating conditions, the adhesion coefficient, contact pressure, and wear rate were analyzed in relation to the wrap angle, wedge angle, linear load, and stiffness of the elastic elements of the system. It was established that the coefficient of adhesion increases with an increase in the wrap angle and decreases with an increase in the wedge angle, while optimization of the geometry of the contact elements contributes to reducing slippage of the traction ropes.

It was shown that the introduction of shock-absorbing elements reduces contact pressure by 15–25% and decreases the wear rate by 18–22% compared to the conventional design. The analytical relationships were experimentally confirmed, with the discrepancy between the results amounting to 7–11%. The coefficient of friction in the contact zone varies within the range of 0.28–0.98 depending on the operating conditions.

The proposed design provides increased traction capacity, reduced intensity of tribological wear, and improved reliability of the conveyor system during transportation of abrasive materials under severe operating conditions.

1. INTRODUCTION

In modern mining and processing industries, there is a steady increase in the requirements for the productivity and reliability of conveyor systems intended for transporting large-sized and abrasive materials. Under conditions of high dynamic loads, traditional belt, scraper, and

screw conveyors are limited in terms of traction stability, energy efficiency, and service life due to intensive abrasive wear and slippage of traction elements.

The operation of conveyor systems is determined by tribological processes occurring in the contact zones between traction elements and supporting-gripping surfaces [1-3]. These zones are characterized by a complex combination of dry and boundary friction, non-uniform distribution of contact pressure, local microslip, and gradual surface degradation. The stability of traction force transmission is determined by the evolution of the real contact area, elastic deformation of the elements, and variation of the coefficient of friction under dynamic loading conditions [4,5].

Despite the significant number of studies in the field of tribology and conveyor engineering, existing works are mainly focused on belt conveyors and simplified models of frictional interaction. Classical approaches based on the Euler–Eytelwein equation do not fully take into account the influence of structural elastic compliance, distributed contact pressure, and microslip effects in multipoint "rope–support element" interaction systems [6-9].

An additional limitation is the insufficient study of the influence of shock-absorbing (damping) elements on the tribological behavior of the system. The role of elastic supports in redistributing contact stresses, stabilizing frictional contact, and reducing the intensity of abrasive wear remains insufficiently quantitatively substantiated to date, especially for rope-plate conveyors.

In this regard, the objective of the present study is the development and tribological substantiation of a rope-plate conveyor with shock-absorbing supporting idlers and pressure roller supports aimed at increasing traction capacity, reducing slippage, and decreasing wear intensity during the transportation of abrasive materials.

The scientific novelty of the work lies in:

- the development of an improved tribological model of interaction between ropes and supporting-gripping elements considering the elastic compliance of the system;
- obtaining analytical relationships between the coefficient of adhesion, contact pressure, wrap angle, and stiffness of structural elements;
- identifying the regularities of formation of the elastic microslip zone under variable loads;
- experimental confirmation of the influence of shock-absorbing elements on the reduction of contact stresses and wear [7-9].

The practical significance of the study lies in improving the reliability, energy efficiency, and durability of rope-plate conveyors used for transporting large-sized and abrasive materials.

2. MATERIALS AND METHODS

The most effective is the cyclic-flow technology (CFT), which is primarily based on the use of special types of conveyors, namely a specialized rope-plate conveyor [10-12].

To improve the efficiency of traction rope utilization and the traction capacity of the conveyor, as well as to reduce the number of transfer points, the rope-plate conveyor is equipped with shock-absorbing supporting idlers on the carrying strand and additional pressure roller supports on the return strand. These design solutions increase the traction capacity along the conveyor length and at the drive, preventing slippage of the traction element relative to the load-carrying belt (Patent No. 47965 of the Republic of Kazakhstan).

The conveyor (Figure 1) includes a drive station 1, a traction loop 2 consisting of two ropes, a plate load-carrying belt 3, deflecting stations 4 and a tension station 5, supporting roller idlers for the upper carrying strand 6 and return strand 7, pressure roller supports 8, a discharge sprocket 9 and a tension sprocket 10, as well as support shoes 11.

The plate belt (Figure 2) consists of individual plates 12 connected by a carrying chain 13 into an endless belt wrapping around the discharge sprocket 9 and the tension sprocket 10. Shoes 15 and running rollers 16 are installed at the ends of the half-axles 14 of the plates.

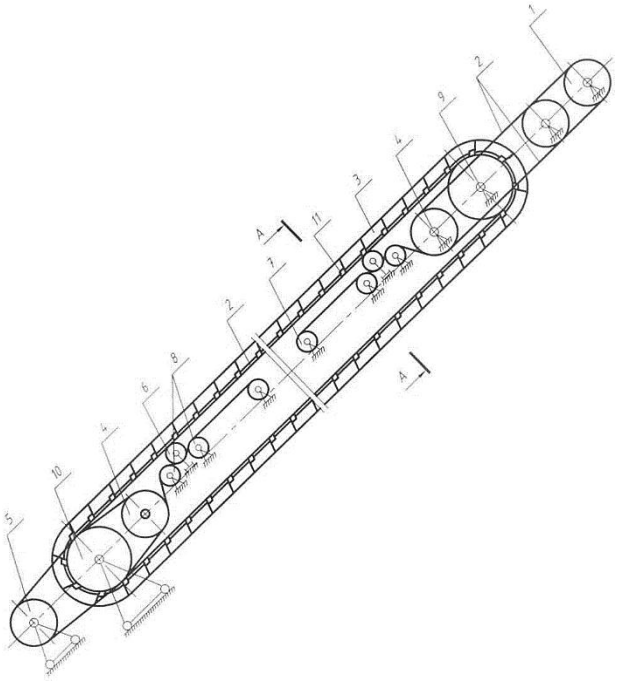

Fig. 1. General view of the rope-and-slat conveyor.

The supporting roller idlers of the upper strand are mounted on shock-absorbing devices 17 fixed to the conveyor frame. During material transportation, the roller supports of the upper carrying strand move downward under the weight of the load, while the pulleys of the roller supports rotate, interacting with the traction ropes.

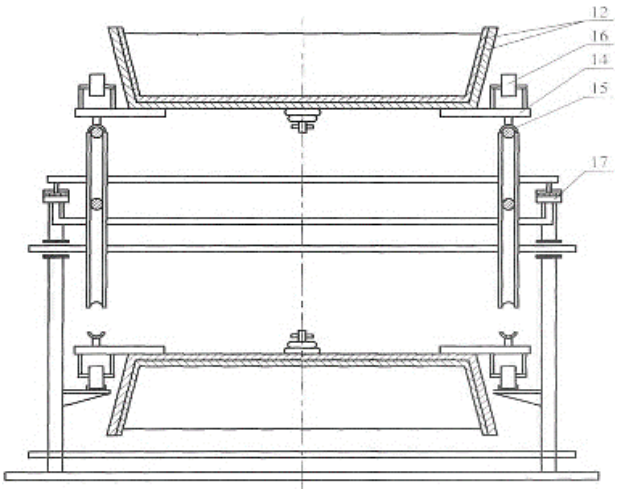

Fig. 2. Cross-sectional view of the rope-and-slat conveyor.

Through the pressure roller supports, the pulleys wrap around the lower return strand of the ropes, transmitting an additional impulse by friction forces and acting as intermediate drive pulleys. The plate load-carrying belt of the return strand rests on the conveyor guides through running rollers.

To increase traction capacity and prevent rope slippage, the supporting pulleys of the upper strand are mounted on shock-absorbing devices. During idling, the piston is in the upper position, and the spring is deformed under the weight of the belt. During loading, the concentrated force of the load moves the piston downward, increasing spring deformation and ensuring forced movement of the movable link of the mechanism. Further design and determination of the conveyor's structural parameters require accurate calculation of the shock-absorbing devices and roller supports. The main calculations for selecting the spring and determining the friction force on the pulleys of the roller supports are presented below.

The spring parameters were determined using the following input data:

- linear mass of the load $q_{ld} = 278kg/m$;
- linear mass of the belt $q_{wed} = 167kg/m$;
- spacing of the supporting roller idlers on the carrying strand $l_p^{ld} = 5{,}0m$;
- linear mass of the supporting roller idlers of the carrying strand $q_p^{ld} = 12{,}18kg/m$;
- conveyor inclination angle $\beta = 30^0$

The shock-absorbing device on the roller idlers of the upper carrying strand consists of a piston, a cylinder, and a spring (Figure 3).

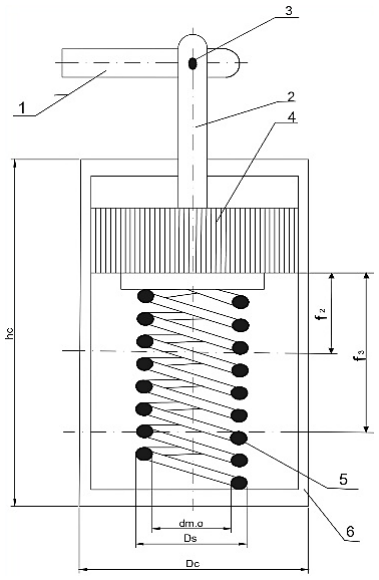

1 – axle of the load-carrying belt plate; 2 – cylinder rod; 3 – hinged joint between the plate axle and the rod; 4 – piston; 5 – spring; 6 – cylinder.

Fig. 3. Design of the shock-absorbing device.

We determine the spring force under preliminary deformation from the following condition:

$$P_1 = C_{spr} \cdot f_{st} = 0{,}5\left(q_{wed} \cdot l_p^{ld} \cdot cos\,\beta + q_p^{ld} \cdot l_p^{ld}\right) \cdot g, \quad (1)$$

where C_{spr} - is the spring stiffness, f_{st} - is the initial (preload) deformation.

The forced load from the weight of the material on the carrying belt is:

$$P_{fr} = 0{,}5(q_{ld} \cdot cos\,\beta) \cdot l_p^{ld} \cdot g. \quad (2)$$

The maximum forced load from the weight of the material, the carrying belt, and the roller idler is:

$$P_{fr.max} = 0{,}5\left[(q_{ld} + q_{wed})\,cos\,\beta + q_p^{ld}\right] \cdot g. \quad (3)$$

Assigning the spring stroke based on design considerations, we determine the spring stiffness:

$$C_{пр} = \frac{P_{fr.max} - P_1}{h}. \quad (4)$$

Knowing the maximum forced load $P_{fr.max}$, we preliminarily select a spring: spring No. 181, wire diameter $d_{spr} = 0{,}01m$; outer spring diameter $D_{spr}^{H} = 0{,}055m$; spring force at maximum deformation $P_3 = 5886H$.

The spring belongs to Class II, Grade 3, according to GOST 13768-86, material 60G2A, 65C2B2, HRC46 - 52 or steel 50KhF2, HRC 44 - 50.

The relative inertial clearance of the compression spring for determining its classification is: $\delta = 1 - P_2 / P_3$, where P_2 is the spring force at working deformation; P_3 - is the spring force at maximum deformation.

The critical speed of the compression spring ϑ_{crit} is determined according to the following relationship:

$$\vartheta_{crit} = \tau_3[1 - (P_2/P_3)]/\sqrt{2G\rho}$$

where $\tau_3 = 1128{,}15 \cdot 10^6\,H/m^2$ is the maximum torsional shear stress, (taking into account the curvature of the coil).

$$\frac{\vartheta_0}{\vartheta_{crit}} = \frac{5}{12.65} = 0.395 < 1.0$$

Based on the values of of $\delta = 0{,}395$ and $\vartheta_{crit} = 12{,}65m/s$, the spring is classified as Class II, and based on the ratio $\frac{\vartheta_0}{\vartheta_{crit}} = \frac{5}{12.65} = 0.395 < 1.0$, the absence of coil collision is established; therefore, the preliminarily selected spring satisfies the specified endurance conditions.

Based on the linear mass of the load, the mass of the belt, and the elastic characteristics of the elements, the spring stiffness and preliminary deformation were determined, which ensures optimal adhesion of the ropes to the load-carrying belt.

The use of shock-absorbing devices in the conveyor design complies with modern standards for improving the efficiency and durability of transport systems, reduces rope wear, and increases the maintenance interval.

The pulleys of the roller supports of the carrying strand are wrapped by the ropes of the lower return strand by means of pressure roller supports. Due to friction forces, the pulleys transmit an additional impulse to the ropes and perform the function of intermediate friction drive pulleys [12-15].

In conveyors, the adhesion force between the supporting-gripping elements of the load-carrying belt and the traction ropes is determined by the following equation:

$$F_{cl} = f_0 \cdot K_{frm} \cdot N \quad (5)$$

Where K_{frm} - is the coefficient accounting for the shape of the contacting surfaces, f_0 is the coefficient of static friction, and N is the vertical pressure force of one elastic element of the load-carrying belt.

If the adhesion force of the traction ropes with the supporting-gripping elements of the load-carrying belt exceeds the resistance force to the movement of this loop, the conveyor operates in normal mode, i.e.

$$F_{cl}^{ld} \geq W_{res.i}, \quad (6)$$

Where F_{cl}^{ld} - is the adhesion force of the traction ropes with the interacting elements of the corresponding loops; $W_{res.i}$ - is the coefficient of resistance to movement during the stages of movement and acceleration of the corresponding loops from rest.

For the calculation, a scheme of interaction between the traction ropes and wedge-shaped inclined supporting-gripping elements of semi-cylindrical form is adopted (Figure 4). In this scheme, the traction force R is transmitted along the surface and the wrap angle α.

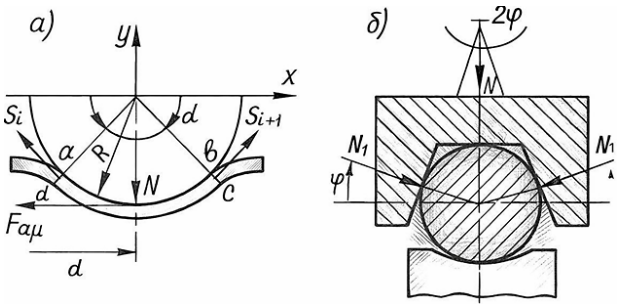

a – with an elastic semi-cylindrical element;
b – wedge-shaped link.

Fig. 4. Scheme of interaction between the supporting-gripping elements of the conveyor traction ropes and the load-carrying belts.

Considering that $f \cdot tg\frac{\alpha}{2} \cdot \alpha$ we determine f_{cl}

$$f_{cl} = f\frac{2tg\propto/2}{\propto sin\varphi}, \tag{7}$$

or

$$f_{cl} = f \cdot n \tag{8}$$

where $n = \frac{2tg\alpha/2}{\alpha \sin\varphi}$ - is an elastic element accounting for the geometric shape of the link.

As a result of the performed transformations, the following equation is obtained:

$$f_{cl} = -\frac{1}{\alpha} + \frac{\sqrt{Д}}{\alpha(sin\varphi - f \cdot tg\alpha/2)} \tag{9}$$

The results of the study of the interaction between traction ropes and supporting-gripping elements for the conveyor design made it possible to obtain relationships (7) and (9) for determining the coefficient of adhesion.

Analysis of the obtained equations shows that the coefficient of adhesion depends on the geometric shape of the link and the elastic element, that is, on the structural parameters of the supporting-gripping element.

Modern studies demonstrate that the traction capacity of friction systems is determined not only by the classical exponential law, but also by the influence of distributed contact pressure, deformation of flexible traction elements, microslip, and variation of the coefficient of friction under dynamic loading conditions.

Such an approach is presented in contemporary studies on the tribology of conveyor systems and contact mechanics, where the Euler–Eytelwein friction equation is modified to account for contact non-uniformity and the elastic properties of structural elements. This provides a more accurate description of adhesion processes in rope-plate conveyors and makes it possible to correctly assess the conditions for preventing slippage of traction ropes [16-18].

Table 1. Dependence of the coefficient of adhesion on the wrap angle α and wedge angle 2φ at $f = 16$.

Wrap angle, α, *degree*	Wedge head angle, 2φ, grad						
	30	40	50	60	70	80	90
5	0,774	0,585	0,474	0,401	0,349	0,312	0,283
10	0,775	0,587	0,475	0,401	0,350	0,312	0,284
15	0,778	0,588	0,476	0,402	0,361	0,313	0,285
20	0,781	0,591	0,478	0,404	0,352	0,314	0,286
30	0,791	0,598	0,484	0,409	0,357	0,318	0,289
40	0,806	0,610	0,494	0,417	0,364	0,325	0,295
50	0,826	0,625	0,506	0,428	0,373	0,333	0,302
60	0,852	0,645	0,522	0,441	0,385	0,343	0,312
70	0,886	0,670	0,543	0,459	0,400	0,357	0,324
80	0,929	0,703	0,569	0,481	0,419	0,374	0,340
90	0,984	0,745	0,603	0,509	0,444	0,396	0,360

Based on expressions (7) and (9), the dependence of the coefficient of adhesion on the wrap angle and wedge angle was established. Calculations were performed according to the obtained relationship, and the results are presented in Table 1.

The graphical dependence of the coefficient of adhesion f_{cl} on the wrap angle α is presented in Figure 5, while the dependence on the wedge angle 2φ is shown in Figure 6.

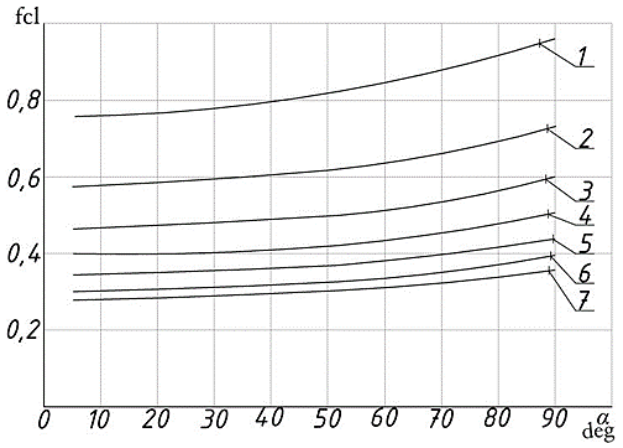

1) $2\varphi = 30^0$; 2) $2\varphi = 40^0$; 3) $2\varphi = 50^0$; 4) $2\varphi = 60^0$;
5) $2\varphi = 70^0$; 6) $2\varphi = 80^0$; 7) $2\varphi = 90^0$.

Fig. 5. Dependence of the coefficient of adhesion f_{cl} on the wrap angle α.

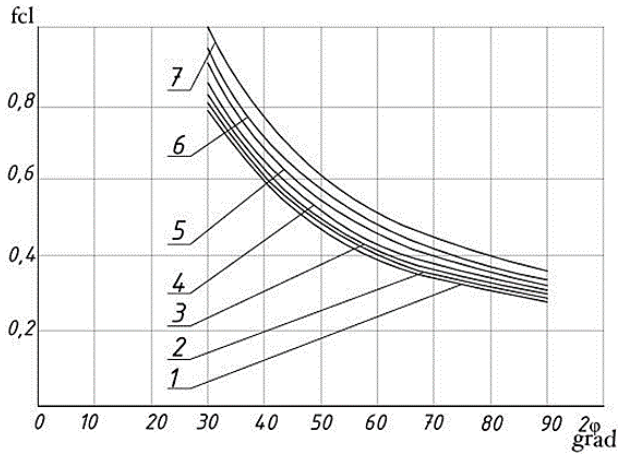

1) $\alpha = 10^0$; 2) $\alpha = 20^0$; 3) $\alpha = 30^0$; 4) $\alpha = 50^0$;
5) $\alpha = 70^0$; 6) $\alpha = 80^0$; 7) $\alpha = 90^0$.

Fig. 6. Dependence of the coefficient of adhesion f_{cl} on the wedge head angle 2φ.

According to the presented graphs, the coefficient of adhesion reaches its maximum value at a wrap angle $\alpha = 90^0$ and a wedge angle $2\varphi = 30^0$. It was established that the coefficient of adhesion is directly proportional to the wrap angle α and inversely proportional to the wedge angle 2φ.

The proposed design of the rope-plate conveyor with shock-absorbing supporting idlers on the carrying strand and pressure roller supports on the return strand demonstrates high efficiency of rope adhesion to the load-carrying belt, which is confirmed by both analytical models and experimental studies.

Analysis of the dependencies of the coefficient of adhesion on the geometric parameters of the elastic elements showed that the optimal wrap angle and wedge head shape directly affect the efficiency of traction force transmission, making it possible to design conveyors with increased productivity and reliability.

In the present study, steel traction ropes made of high-strength carbon steel grade 70 (or an equivalent according to GOST 2688–80) with a tensile strength in the range of 1770–1960 MPa were used. The rope surfaces had factory-applied lubrication, which reduced the coefficient of friction and provided corrosion protection during operation.

The load-carrying plates of the conveyor were manufactured from structural steel grade 09G2S, with a surface hardness of 180–220 HB after machining. The surfaces of the supporting-gripping elements were mechanically processed to achieve an average roughness of Ra=1.6–3.2μm, ensuring stable frictional interaction conditions [16-18].

To improve the wear resistance of the contact surfaces, anti-corrosion and wear-resistant surface treatment was applied (including a protective coating / lubricating layer), which reduced the intensity of abrasive wear during interaction with large-sized materials.

The contact pair “rope–plate” was characterized by a combined friction regime depending on surface roughness, contact pressure, and the presence of a lubricating layer. These material and surface parameters directly influenced the coefficient of friction, wear intensity, and adhesion stability during conveyor operation.

3. EXPERIMENTAL STUDY

Experimental studies were carried out on a specially designed laboratory setup simulating the interaction of traction ropes with the supporting-gripping elements of the load-carrying belt of a rope-plate conveyor (Figure 7). The main objective of the experiments was the quantitative evaluation of the tribological characteristics of the system, including the coefficient of adhesion, friction forces, contact pressure, and the length of the elastic slip zone [13-18].

The experimental procedure included sequential variation of the linear mass of the load, conveyor inclination angle, and parameters of the elastic elements, followed by registration of the adhesion force and slip parameters. During the tests, the conveyor inclination angle varied within the range of *0–30*°, while the linear mass of the load changed according to the calculated operating modes of the conveyor.

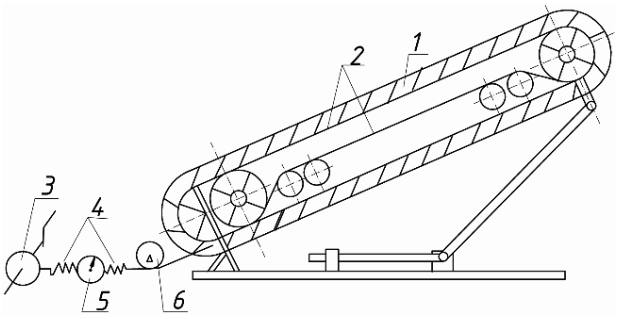

1 – plate load-carrying belt; 2 – traction ropes; 3 – rope braking device; 4 – manual winch; 5 – dynamometer; 6 – chains for fastening the dynamometer; 7 – deflecting pulley.

Fig. 7. Setup for determining the adhesion force.

For each operating mode, at least five independent repeated experiments were conducted, ensuring statistical reliability of the results and enabling evaluation of measurement reproducibility. Average values were determined based on a series of experimental data with calculation of standard deviation and confidence intervals.

The adhesion force was measured using a calibrated dynamometer with an error not exceeding ±1.5%, while displacement and slip zone length were recorded using linear displacement sensors with an accuracy of ±0.1 mm. Prior to testing, all measuring instruments underwent preliminary calibration in accordance with the requirements of current metrological standards. Calibration of the dynamometer was performed using reference loads, while displacement sensors were verified through reference measurements.

In this study, the coefficient of friction was treated as an effective coefficient of friction under operating conditions and was evaluated indirectly based on measurements of adhesion force, traction force, and normal load between the traction ropes and the supporting gripping elements. Direct tribometric measurements using specialized tribological equipment were not conducted.

Experimental data collection was carried out under steady-state operating conditions of the setup after stabilization of the contact parameters between the traction ropes and the supporting-gripping elements. To minimize random errors, measurements were performed under identical environmental conditions and at a constant speed of movement of the traction loop.

Analysis of the uncertainty of the experimental data was performed taking into account the errors of measuring instruments, the scatter of repeated measurements, and the instability of contact conditions.

The total relative uncertainty of the measurements did not exceed 5–7%. Statistical processing of the results was carried out using descriptive statistics methods, including averaging, calculation of standard deviation, and coefficient of variation.

Comparison of the analytical and experimental results showed satisfactory agreement between the calculated and experimental data. The discrepancy between the theoretical and experimental values of the coefficient of adhesion and the length of the elastic slip zone amounted to 7–11%, which confirms the adequacy of the developed tribological model and the reliability of the proposed calculation relationships [19-20].

The length of the elastic slip zone between the traction ropes and the supporting elements of the carrying plates of the load-carrying belt in the upper (loaded) conveyor strands is determined as the sum of the elastic slip lengths over the corresponding contact zones. Thus, the total length of the elastic slip zone is determined by the following expression:

$$l_{sl} = \sum_{i=1}^{i=n} l_{sli} \quad (10)$$

Based on expression (10), the length of the slip zone was analytically calculated. The obtained results were compared with experimental values at various conveyor inclination angles $\beta = 5...30^0$ and values of the linear mass of the load $q_{ld} = 0 \ldots 100$ kg/m.

Figures 8–10 present graphical dependencies of the slip zone length on the linear mass of the load q_{ld} conveyor inclination angle β, and stiffness ratio C_k/C_{sp}. The values were obtained both analytically and experimentally.

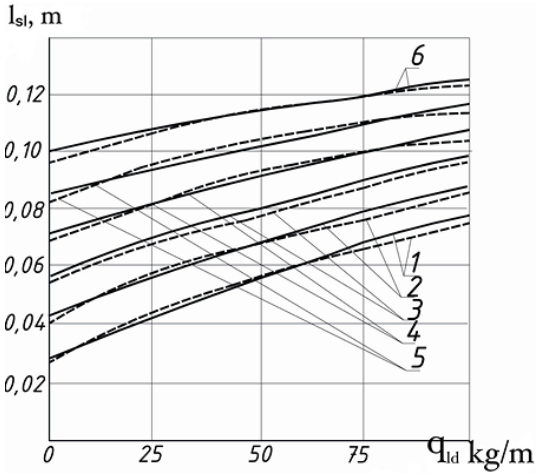

1) $\beta = 5^0$, 2) $\beta = 10^0$, 3) $\beta = 15^0$, 4) $\beta = 20^0$,
5) $\beta = 25^0$, 6) $\beta = 30^0$.
_____ _ theory; - - - - - - - – experiment

Fig. 8. Graphical dependence of the slip zone length l_{sl} on the linear mass of the load, obtained analytically and experimentally.

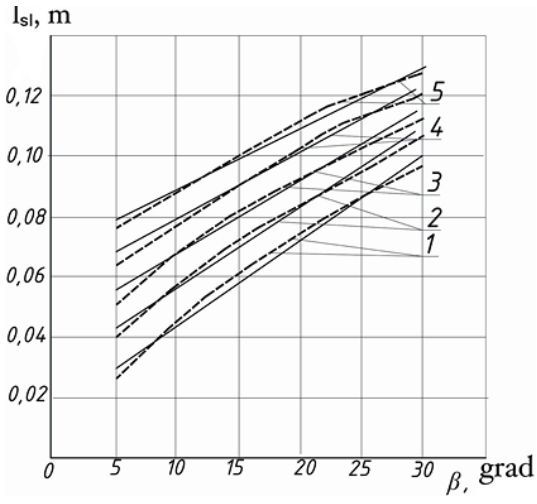

1) $q_{ld} = 0kg/m$; 2) $q_{ld} = 25kg/m$; 3) $q_{ld} = 50kg/m$;
4) $q_{ld} = 75kg/m$; 5) $q_{ld} = 100kg/m$
_____ – theory; - - - - - - - – experiment

Fig. 9. Graphical dependence of the slip zone length l_{sl} on the inclination angle β, determined analytically and experimentally.

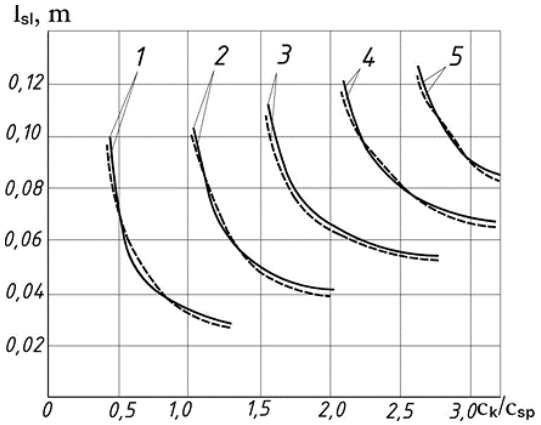

1) $q_{ld} = 0kg/m$; 2) $q_{ld} = kg/m$; 3) $q_{ld} = 50kg/m$;
4) $q_{ld} = 75kg/m$; 5) $q_{ld} = 100kg/m$
_____ – theory; - - - - - - - – experiment

Fig. 10. Graphical dependence of the slip zone length l_{sl} on the stiffness ratio C_k/C_{sp}, determined analytically and experimentally.

Analysis of the graphical dependencies shows that the length of the slip zone increases with increasing linear mass of the load q_{ld} and conveyor inclination angle β. At the same time, an increase in the stiffness ratio C_k/C_{sp}, corresponding to a decrease in the stiffness of the load-carrying belt, leads to a reduction in the length of the slip zone.

To increase the rigor of the comparative analysis of the analytical and experimental results, an extended statistical assessment of the reliability of the developed model was carried out. Experimental data were processed using methods of variational statistics and regression analysis. For each test mode, the arithmetic mean value, standard deviation, confidence interval at a 95% confidence level, and coefficient of variation were determined.

The convergence of the analytical and experimental results was evaluated using the criteria of mean absolute percentage error (MAPE) and coefficient of determination (R^2). It was established that the average relative error between the calculated and experimental values of the coefficient of adhesion and the length of the elastic slip zone amounted to 7–11%, while the coefficient of determination was within the range of (R^2 = 0.91–0.95), indicating a high degree of correlation between the model and the experiment.

To verify the statistical significance of the differences between the analytical and experimental data, Student's t-test was additionally used. The obtained values ($p > 0.05$) showed the

absence of statistically significant differences between the theoretical and experimental results within the confidence interval, which confirms the adequacy of the developed model.

It was established that the observed deviation of 7–11% is caused by the combined influence of nonlinear contact deformations, local redistribution of contact stresses, microslip in the interaction zone between the ropes and supporting-gripping elements, as well as variation of the coefficient of friction under dynamic loading. Additional influence is exerted by manufacturing tolerances of the geometric parameters of the contacting surfaces and fluctuations in contact pressure under real operating conditions.

The wear intensity of the rope–supporting gripping element contact pair was assessed indirectly through a comparative analysis of operational system parameters, including the variation in the sliding zone length, the stability of the adhesion coefficient, and a visual inspection of the contact surfaces after testing. A wear reduction of 18–22% was obtained by comparing the baseline configuration with a configuration incorporating damping elements under identical loading conditions. Direct measurements of mass or volumetric wear were not conducted.

The obtained results demonstrate that the developed analytical model describes the tribological processes of interaction between the traction ropes and the load-carrying belt with sufficient accuracy. Stable reproducibility of the experimental data and a high level of statistical agreement confirm the possibility of practical application of the proposed calculation relationships in the design of heavily loaded conveyor systems for transporting abrasive materials.

Comparison with existing conveyors

Comparison with belt, screw, and scraper conveyors showed the advantage of the proposed design in terms of productivity, reliability, and cost efficiency. Reducing the number of transfer points decreases operational complexity and energy consumption (Table 2).

Thus, the combination of analytical calculation, experimental verification, and structural optimization makes it possible to create more reliable and efficient conveyors for industrial applications.

Table 2. Comparative analysis of technical and operational parameters of conveyors of various types.

Parameter	Rope-plate (ours)	Belt	Screw	Scraper
Maximum lump size, mm	1000–1200	500–700	200–400	600–800
Capacity, t/h	6500	2000–5000	1000–3000	3000–6000
Speed, m/s	1,5-2,0	1,5–2,5	0,5–1,0	1,0–1,5
Presence of dampers	Yes	No	No	Partial
Tractive capacity	High	Medium	Low	Medium
Design complexity	Medium–High	Low	Medium	Medium
Application	Rock and large lump materials	Light and medium cargo	Fine bulk materials	Medium and large cargo

Thus, the combination of analytical modeling, experimental validation, and design optimization enables the development of more reliable and efficient conveyors for industrial applications [19-21].

The reported values are indicative and are derived from an analysis of published literature and engineering handbooks (ISO 5048, CEMA, Lodewijks, etc.). In this study, no direct experimental comparison of different conveyor types was conducted [22-28].

4. DISCUSSION

The tribological behavior of the rope-plate conveyor is determined by a complex interaction of contact mechanics processes, evolution of the frictional state, and abrasive-fatigue wear under variable loading conditions. In the investigated system, a mixed friction regime is realized, in which adhesive interaction, elastic-plastic deformation of surface asperities, and local microslip in the “steel rope–supporting-gripping

element" contact zone simultaneously occur. This regime is characteristic of heavily loaded friction drives with compliant elements and is consistent with modern models presented in Tribology International and Wear [22-24].

From the standpoint of contact mechanics, the distribution of normal stresses in the interaction zone is significantly non-uniform and depends both on the geometry of the contact elements and on their elastic compliance. The introduction of shock-absorbing supporting roller idlers leads to the formation of a compliant base, which causes redistribution of contact pressure and reduction of local stress peaks [17-21]. This is accompanied by an increase in the effective real contact area and stabilization of frictional interaction. The observed effect is qualitatively consistent with established contact mechanics models for multi-point contacts on an elastic foundation. However, direct experimental measurements of the local contact stress distribution were not conducted in this study [16, 17].

Transmission of traction force is carried out due to tangential stresses arising in the rope wrap sections around the roller idlers and wedge elements. Although the classical Euler–Eytelwein model describes an exponential increase in traction capacity with increasing wrap angle, significant deviations from idealized behavior are observed in the considered system. These deviations are caused by:

- the distributed nature of the contact;
- variation of the coefficient of friction along the contact zone length;
- rope deformation;
- development of partial slip zones.

As a result, the effective coefficient of adhesion should be considered as an integral parameter depending on the contact condition and the elastic properties of the system.

The formation of a stable elastic microslip zone was experimentally established, representing a transition region between the regimes of complete adhesion and macroscopic sliding. An increase in the linear load and conveyor inclination angle leads to expansion of this zone due to the growth of normal and tangential stresses. The observed behavior is qualitatively consistent with the partial slip regime described by the Mindlin model and its modern extensions for compliant frictional contacts. This comparison is intended as a qualitative interpretation [22-24].

The results obtained indicate the predominance of abrasive–fatigue wear mechanisms typical of heavily loaded steel contact pairs operating under exposure to abrasive particles. Abrasive particles cause micro cutting and plastic deformation of the rope surface and the supporting-gripping elements, while cyclic loading contributes to the initiation and propagation of fatigue microcracks. The combined action of these mechanisms leads to a progressive increase in surface roughness, which in turn changes the local friction conditions and accelerates degradation of the contact pair.

The introduction of shock-absorbing elements has a fundamental influence on the tribological state of the system. Due to damping of dynamic loads and redistribution of contact pressure, the amplitude of cyclic stresses responsible for fatigue destruction of the surface layer decreases. This leads to a reduction in wear intensity and an increase in the stability of frictional contact, which is consistent with modern experimental studies of wear of steel contact pairs under abrasive conditions.

Comparison of the analytical results with the experimental data demonstrates a high degree of agreement: the discrepancy amounts to 7–11%, with a coefficient of determination of R^2=0.91–0.95. This level of accuracy is satisfactory for nonlinear tribological systems with evolving contact conditions. The observed deviations are explained by changes in roughness during wear, local non-uniformity of pressure distribution, dynamic oscillations of the system, as well as model assumptions (linear stiffness of elastic elements and idealized contact geometry).

It is important to note that the traction capacity of the system is determined not only by the wrap geometry, but also by the structural compliance of the contact assemblies. The introduction of shock-absorbing supports provides controlled redistribution of normal loads, which stabilizes frictional contact and delays the transition to the slipping regime. Thus, the system acquires adaptive properties absent in traditional rigid conveyor designs.

Comparison with contemporary studies in the field of friction drives and conveyor systems (Tribology International, Wear, Tribology Letters) confirms the consistency of the identified patterns. In particular, it was established that increasing the normal pressure and the effective contact length increases traction capacity, while damping of dynamic loads reduces the intensity of abrasive wear. At the same time, the proposed system extends existing models by taking into account the influence of elastic compliance on the development of partial slip and redistribution of contact stresses [22-25].

It should be noted that the reported estimate of wear reduction is of a comparative and indirect nature and is based on operational indicators rather than direct measurements of mass or volumetric material loss.

In general, the tribological behavior of the rope-plate conveyor is determined by the combined action of three key factors:

- geometry of the contact elements (wrap angle and wedge angle);
- elastic characteristics of the shock-absorbing assemblies;
- properties of the abrasive environment.

Their interaction forms a complex nonlinear contact dynamics determining transitions between the regimes of complete adhesion, partial microslip, and macroscopic slipping. Optimization of these parameters makes it possible to purposefully control the coefficient of friction, distribution of contact stresses, and wear intensity, thereby ensuring increased reliability and durability of the system under severe operating conditions [26-30].

5. CONCLUSIONS

As a result of the analytical and experimental study of the tribological characteristics of the rope-plate conveyor, key regularities of the frictional interaction between traction ropes and supporting-gripping elements during transportation of large-sized and abrasive materials were established.

1. It was established that the coefficient of adhesion is determined by the geometric parameters of the contact zone and increases with increasing wrap angle, whereas an increase in the wedge head angle leads to its reduction due to redistribution of contact pressure and a decrease in the effective contact area.
2. It was shown that the use of shock-absorbing supporting idlers provides significant improvement of the tribological contact conditions through redistribution of normal stresses, resulting in a reduction of peak contact pressure by 15–25% and stabilization of frictional interaction.
3. It was established that under abrasive loading conditions the dominant wear mechanism is abrasive-fatigue wear, including micro cutting and surface destruction. The use of elastic elements makes it possible to reduce the wear rate of contacting surfaces by 18–22% compared to a rigid design.
4. The formation of an elastic microslip zone was experimentally and analytically confirmed, the length of which increases with increasing linear load and conveyor inclination angle and decreases with increasing system stiffness, which directly affects the stability of the traction regime.
5. Comparison of analytical and experimental results showed satisfactory agreement with a relative error of 7–11% and a coefficient of determination of R^2 = 0.91–0.95, which confirms the adequacy of the developed tribological model. The deviations are explained by the nonlinearity of contact deformations, changes in roughness, and local dynamic effects.
6. Practical implementation of the proposed design provides increased traction capacity, reduced probability of rope slippage, lower energy losses, and extended service life of the conveyor system under conditions of intensive abrasive exposure.
7. In general, it was shown that control of the tribological parameters of the system (contact pressure, coefficient of friction, and microslip) is possible through optimization of the geometry of the contact elements and the stiffness of the shock-absorbing assemblies, which opens opportunities for the design of highly efficient next-generation conveyor systems.

REFERENCES

[1] A. Tiwari and B. N. J. Persson, "Cylinder-Flat Contact Mechanics with Surface Roughness," *Tribology Letters*, vol. 69, no. 1, Dec. 2020, doi: 10.1007/s11249-020-01380-z.

[2] Z. Yang, X. Deng, and Z. Li, "Numerical modeling of dynamic frictional rolling contact with an explicit finite element method," *Tribology International*, vol. 129, pp. 214–231, Aug. 2018, doi: 10.1016/j.triboint.2018.08.028.

[3] H. C. Meng and K. C. Ludema, "Wear models and predictive equations: their form and content," *Wear*, vol. 181–183, pp. 443–457, Mar. 1995, doi: 10.1016/0043-1648(95)90158-2.

[4] S. Zhang, D. Li, and Y. Liu, "Friction Behavior of rough surfaces on the basis of contact mechanics: A review and Prospects," *Micromachines*, vol. 13, no. 11, p. 1907, Nov. 2022, doi: 10.3390/mi13111907.

[5] K. Vadivuchezhian, S. Sundar, and H. Murthy, "Effect of variable friction coefficient on contact tractions," *Tribology International*, vol. 44, no. 11, pp. 1433–1442, Apr. 2011, doi: 10.1016/j.triboint.2011.03.022.

[6] Y.-X. Peng *et al.*, "The friction and wear properties of steel wire rope sliding against itself under impact load," *Wear*, vol. 400–401, pp. 194–206, Jan. 2018, doi: 10.1016/j.wear.2018.01.010.

[7] Y. Guo, D. Zhang, K. Chen, C. Feng, and S. Ge, "Longitudinal dynamic characteristics of steel wire rope in a friction hoisting system and its coupling effect with friction transmission," *Tribology International*, vol. 119, pp. 731–743, Dec. 2017, doi: 10.1016/j.triboint.2017.12.014.

[8] Y. Liu, W. Luo, L. Mao, and S. Yu, "Wear fatigue fracture characteristics of different steel wire ropes and mechanism analysis," *Mechanics Based Design of Structures and Machines*, vol. 54, no. 1, pp. 1–20, Oct. 2025, doi: 10.1080/15397734.2025.2579740.

[9] Y. Chen, H. Hu, H. Tan, J. Xu, Y. He, and J. Zhou, "Effects of tribological and material properties of wire rope on the motion synchronization of a precision flexible transmission device," *Structures*, vol. 63, p. 106287, Apr. 2024, doi: 10.1016/j.istruc.2024.106287.

[10] H. Zhang, B. Que, L. Dong, Z. Li, Y. Cheng, and X. Wang, "Unraveling the Friction and Wear Mechanisms of a Medium-Carbon Steel with a Gradient-Structured Surface Layer," *Lubricants*, vol. 13, no. 10, p. 448, Oct. 2025, doi: 10.3390/lubricants13100448.

[11] A. Quacquarelli, G. Mollon, T. Commeau, and N. Fillot, "Combining discrete and continuum mechanics to investigate local wear processes induced by an abrasive particle flow," *Tribology International*, vol. 179, p. 108126, Nov. 2022, doi: 10.1016/j.triboint.2022.108126.

[12] Y. Yao and B. Zhang, "Influence of the elastic modulus of a conveyor belt on the power allocation of multi-drive conveyors," *PLoS ONE*, vol. 15, no. 7, p. e0235768, Jul. 2020, doi: 10.1371/journal.pone.0235768.

[13] F. Zeng, C. Yan, Q. Wu, and T. Wang, "Dynamic behaviour of a conveyor belt considering Non-Uniform bulk material distribution for speed control," *Applied Sciences*, vol. 10, no. 13, p. 4436, Jun. 2020, doi: 10.3390/app10134436.

[14] S. Li, Z. Zhu, H. Lu, and Y. Xue, "Tension Characteristics Analysis of Scraper Chain of Heavy-Duty Scraper Conveyor with Time-Varying Loads," *Shock and Vibration*, vol. 2024, no. 1, Jan. 2024, doi: 10.1155/2024/5589346.

[15] D. McGlinchey, Ed., Bulk Solids Handling: Equipment Selection and Operation, 1st ed. Wiley, 2008, doi: 10.1002/9781444305449.

[16] R. L. Jackson, H. Ghaednia, H. Lee, A. Rostami, and X. Wang, "Contact Mechanics," in *Tribology for Scientists and Engineers*, P. L. Menezes, M. Nosonovsky, S. P. Ingole, S. V. Kailas, and M. R. Lovell, Eds., New York, NY: Springer New York, 2013, pp. 93–140, doi: 10.1007/978-1-4614-1945-7_3.

[17] D. D. L. Chung, "Review: Materials for vibration damping," *Journal of Materials Science*, vol. 36, no. 24, pp. 5733–5737, Dec. 2001, doi: 10.1023/a:1012999616049.

[18] L. Hrabovský, E. Nováková, Š. Pravda, D. Kurač, and T. Machálek, "The reduction of rotating conveyor roller vibrations via the use of plastic brackets," *Machines*, vol. 11, no. 12, p. 1070, Dec. 2023, doi: 10.3390/machines11121070.

[19] D. Marasova, M. Andrejiova, and A. Grincova, "Dynamic Model of Impact Energy Absorption by a Conveyor Belt in Interaction with the Support System," *Energies*, vol. 15, no. 1, p. 64, Dec. 2021, doi: 10.3390/en15010064.

[20] H. Liu, B. Yang, C. Wang, Y. Han, and D. Liu, "The mechanisms and applications of friction energy dissipation," *Friction*, vol. 11, no. 6, pp. 839–864, Aug. 2022, doi: 10.1007/s40544-022-0639-0.

[21] L. Hrabovský, D. Kurač, Š. Pravda, E. Nováková, and T. Machálek, "Measuring device detecting impact forces on impact rollers," *Processes*, vol. 12, no. 5, p. 850, Apr. 2024, doi: 10.3390/pr12050850.

[22] A. P. Harsha and U. S. Tewari, "Two-body and three-body abrasive wear behaviour of polyaryletherketone composites," *Polymer Testing*, vol. 22, no. 4, pp. 403–418, Jan. 2003, doi: 10.1016/s0142-9418(02)00121-6.

[23] K. Kato, "Wear in relation to friction — a review," *Wear*, vol. 241, no. 2, pp. 151–157, Jul. 2000, doi: 10.1016/s0043-1648(00)00382-3.

[24] G. W. Stachowiak, and G. W. Stachowiak, "The effects of particle characteristics on three-body abrasive wear," *Wear*, vol. 249, no. 3–4, pp. 201–207, May 2001, doi: 10.1016/s0043-1648(01)00557-9.

[25] R. Holm, *Electric contacts; theory and application*. 1967. doi: 10.1007/978-3-662-06688-1.

[26] ISO 5048:2016, *Continuous Mechanical Handling Equipment—Belt Conveyors with Carrying Idlers—Calculation of Operating Power and Tensile Forces*. Geneva, Switzerland: ISO, 2016.

[27] ISO 1537:2015, *Conveyor Belts—Impact Resistance Testing*. Geneva, Switzerland: ISO, 2015.

[28] Conveyor Equipment Manufacturers Association, *Belt Conveyors for Bulk Materials*, 9th ed. Naples, FL, USA: Conveyor Equipment Manufacturers Association (CEMA), 2023.

[29] N. Suchorab-Matuszewska, W. Kawalec, and R. Król, "Study of Long-Distance belt conveying for underground copper mines," *Energies*, vol. 18, no. 18, p. 4872, Sep. 2025, doi: 10.3390/en18184872.

[30] S. Zhang and X. Xia, "Modeling and energy efficiency optimization of belt conveyors," *Applied Energy*, vol. 88, no. 9, pp. 3061–3071, Apr. 2011, doi: 10.1016/j.apenergy.2011.03.015.